Characterization of Magnesium Silicide Stannide Powder for use in Selective Laser Melting

R. Gray[*,**], and S. LeBlanc[*,**]

[*]Department of Mechanical and Aerospace Engineering
The George Washington University, Washington, DC, 20052
[**]The LeBlanc Lab, Washington D.C., https://www.leblanclab.com/

ABSTRACT

This study examines magnesium silicide stannide ($Mg_2Si_{0.4}Sn_{0.6}$) powder, a thermoelectric material optimal for high temperature applications. Powder morphology and particle size distribution were analyzed through optical microscopy and the image analysis software FIJI. The ability to spread was assessed across 100 µm and 500 µm thick grooves using two rolling techniques, as well as a razor blade. Flowability was examined through the measurements of, angle of repose, angle of spatula, and compressibility. $Mg2Si0.4Sn_{0.6}$ was characterized to establish the feasibility of using this powder in the selective laser melting process

Keywords: magnesium silicide stannide, selective laser melting, thermoelectric generators, powder characterization

1 INTRODUCTION

Thermoelectric generators (TEGs) are solid state devices which convert waste heat from various heat systems into usable electricity. Current advances in thermoelectric materials have not resulted in efficient and economically viable devices due to manufacturing challenges. The current manufacturing process requires many steps before assembly. These steps not only create a lengthy time process and material waste, but they also provide limited geometries (rectangular legs only) which fail to effectively capture waste heat from curved heat systems.

Selective laser melting (SLM) is an additive manufacturing technique which has the potential to combat challenges that current manufacturing options face. During SLM a layer of powder is spread onto the powder bed. This layer is scanned by a laser in a desired pattern, sintering, or melting the powder particles together. Another layer of powder is spread, and the process is repeated until the desired structure is formed. The remaining powder is then removed and recycled for the next device. This process; however, requires specific starting powder characteristics: desired particle size distribution, and high levels of circularity and convexity. Selective laser melting has been used in the manufacturing of metal and ceramic devices; however, has not been shown with semiconductor materials such as those used for thermoelectrics.

Powder parameters such as convexity, circularity, and particle size distribution (PSD) not only effect the flowability through the SLM process but also the density of the final thermoelectric device. With a higher density, TEGs are more efficient and are more resilient to internal fractures. If particles are elongated and nonuniform, there is an increase in particle friction and possible particle interlocking which in return decreases spreadability and flowability. These characteristics also decrease the final density as they can lead to uneven sintering, and interlayer voids, which cause internal fractures [1].

2 METHODS AND RESULTS

2.1 Powder Preparation

The $Mg_2Si_{0.4}Sn_{0.6}$ powder was prepared with a mortar and pestle. Solid $Mg_2Si_{0.4}Sn_{0.6}$ disks were ground in an inert argon atmosphere with levels of O_2 and H_2O at ~0.5 ppm and a pressure maintaining between 2-5 mbars. The disks were crushed until the powder was below 212 µm in diameter (d_p). Figure 1 shows an optical microscope image of the prepared powder.

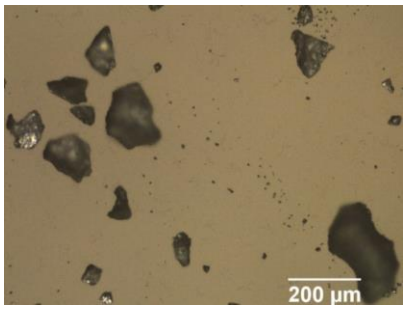

Figure 1. Optical Microscope image (10x) of $Mg_2Si_{0.4}Sn_{0.6}$ $dp < 212$ µm. Showing a wide PSD with many jagged edged and elongated particles.

2.2 PSD and Morphology

To characterize PSD, circularity, and convexity, optical microscopy was used. 0.1g of $Mg_2Si_{0.4}Sn_{0.6}$, $d_p < 212$ µm, powder was mixed with 5ml of ethylene glycol. This suspension was spin coated onto glass slides over three steps. Step one was for 10 seconds at 1200 rpm, step two was for 45 seconds at 1600 rpm, and step three was for 10

seconds at 1200 rpm. A total of 50 images were taken from the three samples.

Once the images were acquired, they were all processed through an ImageJ software derivative called Fiji Is Just ImageJ (FIJI) [2]. In the program, each image was converted to 8-bit greyscale and then its contrast was enhanced. Following this, a mask was applied over the image, inverting the look-up table (LUT) and producing a flat black and white image. Additionally, scale was applied to each image in microns. Utilizing the black and white image, the particles were then analyzed to obtain values for area, perimeter, Ferret's diameter, and convex perimeter. To obtain the convex perimeter, a plugin was applied to FIJI called "Shape Filter" [3]. A macro was utilized to automate the process and to help control for human error.

PSD looks at the different sizes of particles that are represented in a sample. This measurement is based on Ferret's diameter which is the longest diameter at any point on the particle. A wider PSD decreases spreadability and flowability as there is an increase in interparticle friction and interparticle locking. This creates a challenge for manufacturing. However, a narrower PSD decreases the final density of the device by increasing the number of pores [1]. This in return causes a challenge for the end product. Finding an optimal balance between these two parameters is key to manufacturing and producing effective TEGs.

A wide right skewed PSD, with an average particle size diameter of 27.79 µm, was seen. This is due to the way that the $Mg_2Si_{0.4}Sn_{0.6}$ disks are crushed. Which negatively impacts the circularity and convexity of the powder.

Circularity is a ratio of area to Ferets diameter squared. It examines how elongated or circular a particle is and is on a scale from zero to one. A ratio of one being the most circular and zero the most oblong. Convexity is a ratio of convex perimeter to perimeter. It defines how abstract or rough a particle is and is also on a scale from zero to one. A ratio close to zero indicating a very abstract shape with many sharp edges and points, and one denoting a perfectly smooth and round particle.

The circularity results depicted a normal distribution with an average of 0.57, which is a medium value. Particles with low circularities lead to decreased spreadability and flowability as well as create uneven powder beds. The convexity results were skewed to the left with an average value of 0.89, which is good. Particles with higher convexity values will have decreased interparticle locking and will create a more uniform powder bed.

The initial preparation of the powder produced a wide PSD. The optimal PSD will need to be chosen in order to produce effective TEG's and help to improve the flowability and spreadability of the powder during the SLM process. Irregularities in the powder's morphology will also need to be improved to maximize the potential for the powder to spread and flow by decreasing interparticle locking and interparticle friction.

2.3 Spreadability

Spreadability, or the quality of how powder spreads, was examined on 100 µm and 500 µm grooved stainless steel plates. Three different spreading techniques were used: forward rolling, counter rolling, and spreading with a razor blade. Seven different nominal sieve sizes were evaluated: $d_p < 212$ µm, 150 µm $< d_p <$ 212 µm, 106 µm $< d_p <$ 150 µm, 75 µm $< d_p <$ 106 µm, 53 µm $< d_p <$ 75 µm, 46 µm $< d_p <$ 53 µm, $d_p <$ 46 µm. All spreading took place in a fume hood, and consisted of one sweep or roll with a consistent medium pressure across the entire surface. Each spread was conducted three times to evaluate repeatability. This is seen in Figure 2, were the picture on the left is of the whole grooved plate and the picture on the right is an optical microscope image at 5x magnification.

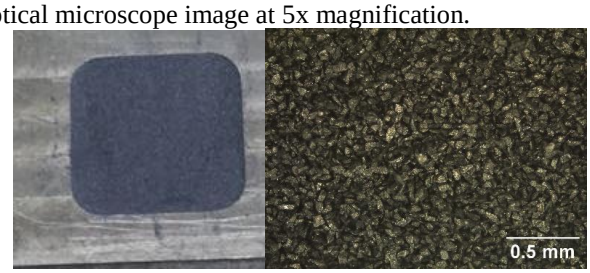

Figure 2. Counter rolled on a 500 μm groove with $46\ \mu m < dp < 53$ µm powder. Excellent Spreadability. spread fully across with no excess on the sides. Very good compaction with very few gaps. Very even surface quality, with very low height variation between layers. Small amount of agglomeration noticed.

Spreadability is affected by interparticle locking, which is directly related to PSD, circularity, and convexity. As you decrease PSD, and increase circularity and convexity values, spreadability will increase. The SLM process creates devices through spreading, and sintering layers of powder. To obtain perfectly sintered layers during the SLM process each layer must be densely packed and have a uniform thickness.

Spreading trials were very repeatable, with all three trials producing identical images for each of the seven nominal sieve sizes respectively. Spreading with a blade or counter rolling across the 500 µm groove produced good uniformity and packing density. The best trial was 46 µm $< d_p <$ 53 µm powder counter rolled, as seen in Figure 2. Spreading across the 100 µm groove produced poor results. The best was also 46 µm $< d_p <$ 53 µm powder counter rolled; however, there were still gaps and some surface irregularities.

As nominal sieve size decreased packing density and surface uniformity increased. However, as nominal sieve size decreased, agglomeration increased, causing cracks in the powder bed. Across all seven nominal sieve sizes and with both the 100 µm and 500 µm grooves, forward rolling created the best compressibility. But, it did not achieve the correct layer size and took more powder to spread fully across. Spreading with a blade and counter rolling both had very similar results across all trials, with counter rolling

attaining a slightly better surface uniformity and packing density. For spreading across the 100 µm groove these two techniques produced layers with minimal powder and very little packing; however, across the 500 µm groove they both created a uniform and highly compact layer, with little to no gaps in the powder bed.

With a thicker groove and having the nominal sieve size of the particles be smaller than the groove depth, the particles can form more than one layer. The increase in the number of layers of particles increases the surface area in which the particles are in contact with each other. The increase in contact area decreases the number of particles that are picked up off the surface through spreading. Decreasing the number of gaps or voids in the powder bed and increasing the packing density and surface uniformity. The increase in packing density and surface uniformity, is key for producing effective TEGs; however, a thicker layer size is worse for sintering, as there can be incomplete melting between layers and balling on the device's surface [4]. Illustrating again the tradeoff between optimizing manufacturing parameters and the performance of the end product.

2.4 Flowability

Flowability is multidimensional and depends on many powder characteristics. Because of this, it is important to look at many measurements when assessing the flowability of a powder. These measurements include angle of repose, angle of spatula, and compressibility. Each of these measurements helps to paint a picture of how the powder will act throughout the manufacturing process.

Measurments for angle of repose, angle of spatula, and compressability follow the Unites States Pharmacopeia (USP) powder flowability index [5]. This is a way to quantitatively evaluate the flowability of a powder, through each individual measurement.

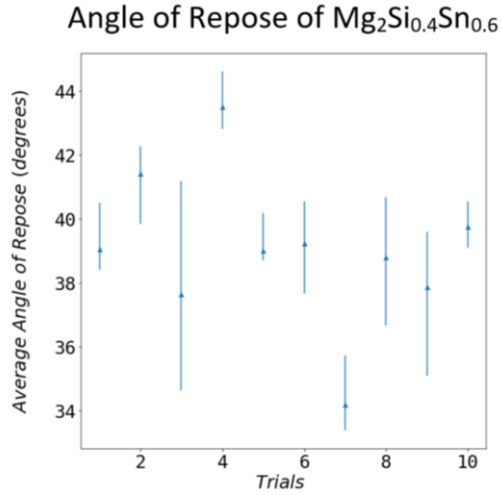

Figure 3. Average angle of repose measurements and variation in the averages across ten trials for $Mg_2Si_{0.4}Sn_{0.6}$ $dp < 212$ µm, the average angle being 39.03°, indicating fair flowability.

To measure angle of repose 10g of $d_p < 212$ µm powder was used. The powder flowed through a funnel held one inch above the measuring surface until all the powder formed a conical pile. The angle between the horizontal plane and the top of the pile is the angle of repose. Five measurements were taken from ten separate trials and were conducted in a fume hood. The measurements were taken using the mobile app, Angle Measure Tool [6].

Seen in Figure 3 the averge angle of repose is 39.03° which according to the USP flowability index is an indication of fair floawbility. The smaller the angle, the better the flow of the powder. PSD, circularity and convexity all influence angle of repose. With a wider PSD, angle of repose increases, indicating poor flowabiltiy. Greater values for circularity and conexity result in a smaller angle of repose, signaling good flowabiltiy [5].

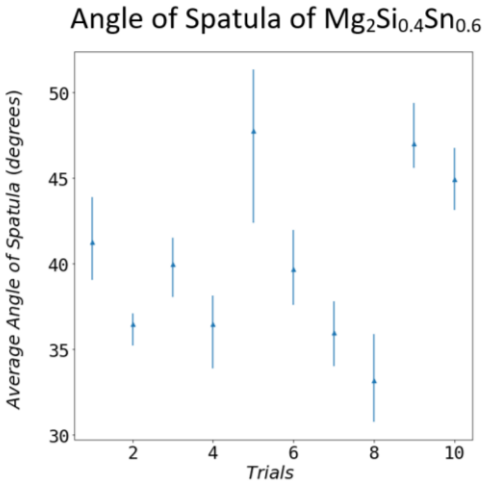

Figure 4. Average angle of spatula measurements and variation in the averages across ten trials for $Mg_2Si_{0.4}Sn_{0.6}$ $dp < 212$ µm, the average angle being 40.23° indicating fair flowability.

To measure angle of spatula, a spatula is placed into a pile of powder, and when fully covered in powder lifted vertical up. The angle between the horizon and the top of the pile is the angle of spatula. A 10g conical pile of $d_p < 212$ µm powder was used. Five measurements were taken from ten trials and were conducted in a fume hood. The measurements were taken using the mobile app, Angle Measure Tool [6].

The average angle of spatula is 40.23° as seen in Figure 4. Which according to the USP flowability index, indicates fair flowability. The larger the angle of spatula the better the flow of the powder. PSD, circularity, and convexity also directly relate to the angle of spatula. A narrower PSD will cause a smaller angle of spatula, indicating good flow. Low values of circularity and convexity will result in a larger angle of spatula signaling poor flowability [5].

Compressibility is the ratio of tapped density to bulk density. Compressibility was examined across 7 nominal sieve sizes: $d_p < 212$ µm, 150 µm $< d_p < 212$ µm, 106 µm $< d_p < 150$ µm, 75 µm $< d_p < 106$ µm, 53 µm $< d_p < 75$ µm, 46 µm $< d_p < 53$ µm, $d_p < 46$ µm. To measure bulk density 0.3g

of powder was carefully poured into a graduated cylinder, making sure the powder didn't compress. The mass of the powder was then taken, and the bulk density calculated. The top of the graduated cylinder was then tapped with a metal spatula for 60 seconds, until the powder no longer compressed. The change in volume was recorded and any change in mass was noted. Using the new volume and mass the tapped density was calculated. Each measurement was taken three times for five separate trials for each of the nominal sieve sizes.

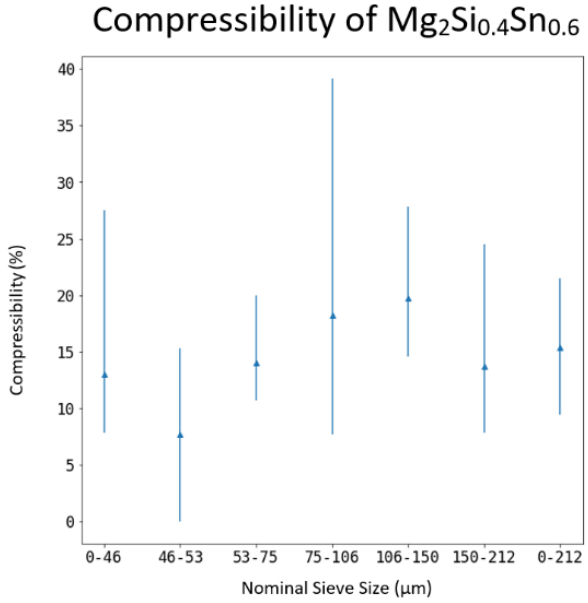

Figure 5. Average compressibility values and variation in measurements for $Mg_2Si_{0.4}Sn_{0.6}$ across seven nominal sieve sizes. dp< 212 µm, and 150 µm < dp< 212 µm indicates fair flowability. 106 µm < dp< 150 µm, 75 µm < dp< 106 µm, 53 µm < dp< 75 µm, and dp< 46 µm indicates good flowability. 46 µm < dp< 53 µm indicates excellent flowability.

The averages, shown in Figure 5, for the d_p< 212 µm, and 150 µm < d_p< 212 µm powder indicated fair flowability according to the USP flowability index. The 106 µm < d_p< 150 µm, 75 µm < d_p< 106 µm, 53 µm < d_p< 75 µm, and d_p< 46 µm powder averages showed good flowability based on the USP flowability index. And the best flowability was the 46 µm < d_p< 53 µm powder, who's average indicated excellent flow as specified by the USP flowability index.

The smaller the difference between tapped and bulk density the better the flowability [5]. As circularity and convexity values increase the compaction of the powder decreases, which increases flowability. This is due to decreased points of contact between particles and a decrease in interparticle locking. If the PSD of the powder is narrower there will also be less compaction, producing a better flowability. This is a result of a decrease in smaller particles filling in the gaps created by bigger particles.

Overall the powder had fair flowability with all nominal sieve sizes below 150 µm in diameter showing good flowability and 46 µm < d_p< 53 µm powder showing excellent flowability. This matches with initial observations of watching the powder flow in a vial.

3 ERROR

Spreadability and flowability tests were not conducted in an inert atmosphere. Minor oxidation was seen as $Mg_2Si_{0.4}Sn_{0.6}$ is reactive with oxygen. Because the environment was not controlled the powder was also exposed to other air contaminants and humidity. The environment was however, kept relatively the same across all the experiments included in this report. The oxidation and potential contamination may have caused increased interparticle locking and interparticle friction which may mean that if the experiments were repeated under different conditions the results may not yield the same.

4 CONCLUSION

$Mg_2Si_{0.4}Sn_{0.6}$ powder was characterized by PSD, circularity, convexity, spreading tests, angle of repose, angle of spatula, and compressibility. In order to understand how the powder would act in the SLM process. Optimizing PSD and decreasing irregularities in particle morphology will need to be overcome before $Mg_2Si_{0.4}Sn_{0.6}$ can effectively create TEGs. However, given the results certain nominal sieve sizes show good flowability and spreadability indicating $Mg_2Si_{0.4}Sn_{0.6}$'s potential for success in the SLM process.

REFERENCES

[1] Ahmed El-Desouky, Michael Carter, Mohamed Mahmoudi, Alaa Elwany, Saniya LeBlanc. "Influences of energy density on microstructureand consolidation of selective laser melted bismuth telluride thermoelectric powder". *Journal of Manufacturing Processes*, vol. 25, pp.

[2] Wagner, T and Lipinski, H 2013. IJBlob: An ImageJ Library for Connected Component Analysis and Shape Analysis. Journal of Open Research Software 1(1):e6, DOI: http://dx.doi.org/10.5334/jors.ae

[3] Schindelin, J.; Arganda-Carreras, I. & Frise, E. et al. (2012), "Fiji: an open-source platform for biological-image analysis", *Nature methods***9(7)**: 676-682, PMID 22743772, doi:10.1038/nmeth.2019 (on Google Scholar).

[4] Batista, N. *et al.* Powder Metallurgy Characterization of Thermoelectric Materials for Selective Laser Melting. *Informatics, Electronics and Microsystems TechConnect Briefs* 166–169 (2017).

[5] Pierre Schuck, Romain Jeantet, Anne Dolivet, "Ch. 8 Determination of Flowability and Floodability Indices," in *Analytical Methods for Food and Dairy Powder*, ed 1: John Wiley & Sons Inc., 2012, ch. 8, pp. 129-136.

[6] Shyam, A. *Angle Measure Tool*. Indian Orthopedic Research Group, 2018.